

Performance of Receiver Autonomous Integrity Monitoring (RAIM) for vertically guided approaches

Anaïs Martineau, Christophe Macabiau, Igor Nikiforov, Benoit Roturier

► **To cite this version:**

Anaïs Martineau, Christophe Macabiau, Igor Nikiforov, Benoit Roturier. Performance of Receiver Autonomous Integrity Monitoring (RAIM) for vertically guided approaches. ENC-GNSS 2008, Conférence Européenne de la Navigation, Apr 2008, Toulouse, France. 2008. <hal-01022206>

HAL Id: hal-01022206

<https://hal-enac.archives-ouvertes.fr/hal-01022206>

Submitted on 30 Sep 2014

HAL is a multi-disciplinary open access archive for the deposit and dissemination of scientific research documents, whether they are published or not. The documents may come from teaching and research institutions in France or abroad, or from public or private research centers.

L'archive ouverte pluridisciplinaire **HAL**, est destinée au dépôt et à la diffusion de documents scientifiques de niveau recherche, publiés ou non, émanant des établissements d'enseignement et de recherche français ou étrangers, des laboratoires publics ou privés.

Performance of Receiver Autonomous Integrity Monitoring (RAIM) for Vertically Guided Approaches

A. Martineau¹, C. Macabiau¹, I. Nikiforov², B. Roturier³

¹*Ecole Nationale de l'Aviation Civile, Toulouse, France*

²*Université Technologique de Troyes, Troyes, France*

³*Direction Générale de l'Aviation Civile, Toulouse, France*

BIOGRAPHY

Anaïs Martineau graduated in July 2005 as an electronics engineer from the Ecole Nationale de l'Aviation Civile (ENAC) in Toulouse, France. She is now working as a Ph.D. student at the signal processing lab of the ENAC where she carries out research on integrity monitoring techniques.

Christophe Macabiau graduated as an electronics engineer in 1992 from the ENAC in Toulouse, France. Since 1994, he has been working on the application of satellite navigation techniques to civil aviation. He received his Ph.D. in 1997 and has been in charge of the signal processing lab of the ENAC since 2000. His research now also applies to vehicular, pedestrian and space applications, and includes advanced GNSS signal processing techniques for acquisition, tracking, interference and multipath mitigation, GNSS integrity, as well as integrated GNSS inertial systems and indoor GNSS techniques.

Igor Nikiforov received his M.S. degree in automatic control from the Moscow Physical-Technical Institute in 1974, and the Ph.D. in automatic control from the Institute of Control Sciences (Russian Academy of Science), Moscow, in 1981. He joined the University of Technology of Troyes (UTT) in 1995, where he is Professor and Head of the Institute of Computer Sciences and Engineering of Troyes. His scientific interests include statistical decision theory, fault detection/isolation/ reconfiguration, signal processing and navigation.

Benoît Roturier graduated in Engineering from the ENAC in 1985 and obtained a PhD diploma in Electronics from Institut National Polytechnique of Toulouse in 1995. His activities are within the France aviation administration (DGAC) since 1987, where he has been successively managing installation of Instrument Landing Systems (ILS) at STNA, head of the research laboratory on CNS systems of ENAC, head of satellite navigation subdivision (GNSS) within DSNA/DTI (Direction des Services de la Navigation Aérienne/Direction de la Technique et de l'Innovation). Since 2007, he is the project manager of satellite navigation (GNSS) and area navigation (RNAV) implementation for DSNA/DTI.

INTRODUCTION

Receiver Autonomous Integrity Monitoring (RAIM) is a simple and efficient solution to check the integrity of GNSS in civil aviation applications such as Non Precision Approaches (NPA). In the next ten years, in a multi constellation context implying a large number of satellites and new signals, more demanding phases of flight such as Approach with Vertical guidance (APV) operations could be targeted using RAIM to check GNSS integrity. Considering those expectations, it is needed to precisely determine what are the vertically guided approaches that can be achieved.

Globally, the improvement in the number and quality of measurements (dual frequency measurements, better clock and ephemeris information, better ranging signals) enhances position estimation and autonomous integrity monitoring performance. However, the benefit for position integrity needs to be quantified, as a larger number of available measurements also implies a larger number of potential faulty measurements for the receiver. Moreover, the targeted phases of flight are characterized by smaller horizontal and vertical tolerable position errors compared to NPA, and by lower acceptable probabilities for the corresponding alert limits to be exceeded. Therefore, the threatening range errors that need to be detected by the fault detection algorithm have to be reconsidered, since they could have smaller amplitude, and a probability of occurrence that is not clearly defined currently.

The aim of this study is to evaluate the potential of GPS/Galileo RAIM for APV operations. This paper investigates the extent to which the augmentation of the number of satellites and the improvement of pseudorange measurements quality could enable the use of RAIM for both horizontal and vertical guidance.

The paper is organized as follows. In a first part, every assumption that has been made for this study is reviewed. Thus target operational requirements are formulated and particularly the way these requirements are interpreted to obtain the probability of missed detection is detailed. The way RAIM performance is evaluated is also recalled, and a complete set of models and values are proposed. In particular, measurements quality parameters such as the

UERE are discussed. Then a second part recalls some RAIM techniques such as classical least square residual algorithm and solution separation method. The last part of the study is dedicated to GPS/Galileo RAIM simulations that have been conducted using a proposed pseudorange model of smoothed GPS L1/L5 and Galileo E1/E5b measurements. The different RAIM algorithms previously described are evaluated comparing their performance to achieve operations with vertical guidance.

I- SET OF ASSUMPTIONS THAT HAVE BEEN ADOPTED

I-1 Expected performance bounds

For those RAIM simulations, operations with vertical guidance are targeted and more particularly APV I operations which requirements are described in the following table.

APV I		
Alert limits	Integrity risk	Maximum allowable false alert rate
HAL=40 m VAL=50 m	$2 \times 10^{-7}/150s$ $\cong 1.33$ $\times 10^{-9}$ per sample	1.6×10^{-5} per sample

But other inputs are necessary to monitor GNSS integrity with RAIM algorithms such as the targeted probability of missed detection that depends on the probability of satellite failure. This aspect refers to the threat model and particularly needs to be detailed.

I-1-1- Probability of satellite failure

Two main types of probabilities are available to characterize GPS satellite failure probability:

- the probability of occurrence of satellite failure larger than 30 m (Major Service Failure) which corresponds to 3 events per year [1]

- the probability of occurrence of satellite failure larger than 3.6 m which is $P_f = 4.3 \times 10^{-6}$ per approach per satellite [2], corresponding for an average of 17 visible satellites to $P_{f,17} = 1.75 \times 10^{-3}/h$

First of all, we need to know the minimal amplitude of single pseudorange failure that leads to an unacceptable positioning error for APV I operations and thus the minimal bias amplitude that needs to be detected by RAIM algorithms.

A fault γ is considered as a horizontal positioning failure if its impact violates the integrity risk, that is to say if:

$$(1 - P_f)P_0(\|X_H - \hat{X}_H\| > HAL) + P_f P_\gamma(\|X_H - \hat{X}_H\| > HAL) > P_{Int}$$

A fault γ is considered as a vertical positioning failure if its impact violates the integrity risk such as:

$$(1 - P_f)P_0(|X_V - \hat{X}_V| > VAL) + P_f P_\gamma(|X_V - \hat{X}_V| > VAL) > P_{Int}$$

where P_f is the probability of failure of one satellite
 P_0 corresponds to the fault free case
 P_γ corresponds to the faulty case

Critical biases calculation is done for a given user position at a given moment by:

- Computing the probability to exceed the alert limit in the fault free case $P_0(\|X_H - \hat{X}_H\| > HAL)$ and $P_0(|X_V - \hat{X}_V| > VAL)$

- For each available pseudorange measurement, computing the smallest additional bias b_i that lead to a probability $P_{b_i}(\|X_H - \hat{X}_H\| > HAL)$ or $P_{b_i}(|X_V - \hat{X}_V| > VAL)$ such as:

$$(1 - P_f)P_0(\|X_H - \hat{X}_H\| > HAL) + P_f P_{b_i}(\|X_H - \hat{X}_H\| > HAL) = P_{Int}$$

$$(1 - P_f)P_0(|X_V - \hat{X}_V| > VAL) + P_f P_{b_i}(|X_V - \hat{X}_V| > VAL) = P_{Int}$$

The computations of the probabilities P_0 and P_{b_i} are detailed in appendix and do not depend on any detection algorithm. But it can be seen that they depend on the failure probability of occurrence.

Considering a double constellation GPS/Galileo and APV I requirements, critical biases have been computed for a probability of satellite failure occurrence of $2 \times 10^{-3}/h$ (corresponding to the category of small failures), the smallest obtained values are represented on the following figure:

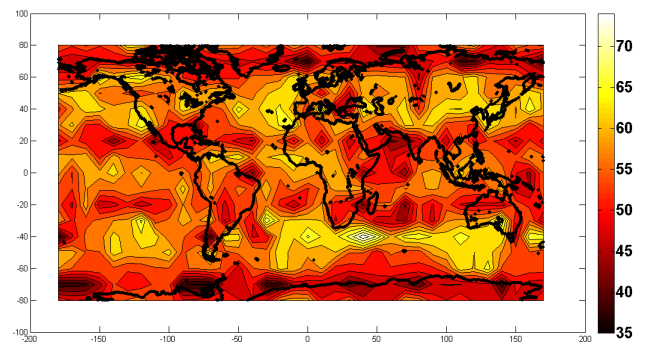


Figure 1- Smallest Critical Bias for APV I operations $P_{f17,1} = 2 \times 10^{-3}/h$

Therefore only considering the single failure case, it can be seen that the smallest single pseudorange failures that lead to an unacceptable positioning error for a probability of occurrence of $2 \times 10^{-3}/h$ are between 35 and 70 meters. These critical biases systematically have an amplitude larger than 30 m and belong to the « Major Service Failure » category, that is to say a signal in space ranging error exceeding 30 meters.

This is why only Major Service Failure events are considered for this study and this assumption leads to the following process.

Let's us denote p the individual major satellite failure probability and N the number of satellite in view, then the probability of having k simultaneous failures among N satellites is:

$$P_{\text{major satellite failure},N,k} = C_N^k p^k (1-p)^{N-k}$$

According to the GPS signal specification 3 major failures are allowed per year and per constellation which correspond to 3.42×10^{-4} major failure per hour for a constellation of 24 satellites such as:

$$P_{\text{major satellite failure},24,1} = 24 p = 3.42 \times 10^{-4}/h$$

$$p = 1.43 \times 10^{-5}/h$$

It is assumed that a Galileo satellite will have the same probability of failure than a GPS satellite.

For a dual constellation, if 20 satellites are in view, the probability of one satellite failure is:

$$P_{\text{major satellite failure},20,1} = 2.85 \times 10^{-4}/h$$

For a dual constellation, if 17 satellites are in view, the probability of one satellite failure is:

$$P_{\text{major satellite failure},17,1} = 2.43 \times 10^{-4}/h$$

Considering this probability of satellite failure occurrence of $2.43 \times 10^{-4}/h$, critical biases have been computed again and the smallest obtained values are represented on the following figure:

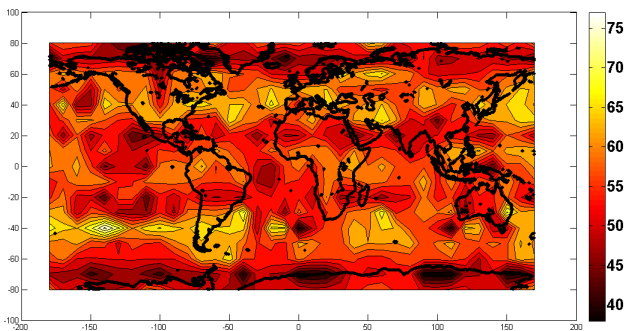


Figure 2- Smallest Critical Bias for APV 1 operations $P_{f,17,1} = 2.43 \times 10^{-4}/h$

Thus it can be verified that the smallest single pseudorange failure that lead to an unacceptable positioning error for a probability of occurrence of $2.43 \times 10^{-4}/h$ are between 40 and 75 meters and that they effectively belong to the « Major Service Failure » category.

I-1-2- Probability of missed detection

Only considering the single failure case, the probability of missed detection P_{md} shall be lower than the integrity risk requirement divided by the probability of failure of one satellite among the all satellites in view.

For example if 17 satellites are in view:

$$P_{md} = \frac{P_{int}}{P_{\text{major satellite failure},17,1}}$$

and finally:

$$P_{md} = 0.0099$$

For this study, the same probability is allocated for vertical and horizontal failure, the integrity risk that it is taken into account in this formula is 1×10^{-7} per approach for the vertical risk and 1×10^{-7} per approach for the horizontal one.

I-2 Performance evaluation

Two types of RAIM algorithm have been tested: the classical LSR RAIM and the Solution Separation RAIM. The way they are implemented is detailed in section II.

As it will be detailed in section II, RAIM tests are built to detect failures that are abnormally large above the assumed noise level. The smallest bias that the test can detect is then projected in the position domain to finally obtain the protection level. It has been decided for this study to also observe the test ability to detect dangerous biases and thus to measure the effective P_{md} . This is why RAIM availability has been observed through two methods:

- Horizontal and Vertical Protection Level have been computed and compare to the corresponding Alert Limit
- Critical biases of size presented in the lat section have been added to pseudo range measurements through Monte Carlo simulations and the capacity of RAIM algorithm to detect them has been measured

Concerning the Monte Carlo simulations, for every user position at every epoch simulation period, critical biases have been successively added on each available measurement. Only one critical bias was added at the same time on the measurements. For each pseudorange, the number of simulation iterations has been designed to be significant with respect to required probability of missed detection such as:

$$n_{iter} \approx 10^{P_{md}^{-1}}$$

In this way, the P_{md} is estimated with a number of digits equal to the number of digits of the required P_{md} .

RAIM function that has been tested was fault detection function.

Simulations have been made for a user grid with a latitude step of 10° and a longitude step of 10° . For each

position of the user grid, a test has been made every 30 minutes.

Each Galileo satellite has an approximate period of 14 hours and 25 minutes which corresponds to 5 revolutions in three days. Three days also correspond to 6 GPS satellites periods. Therefore the simulation time of three days has been chosen.

This represents a total of 49248 different satellite-user geometries to compute protection levels and to test critical bias detection capability.

I-3 Internal RAIM parameters

I-3-1- Geometrical considerations, Position solution estimation

Satellite Constellations that have been considered are an optimized 27 satellites Galileo constellation and an optimized 24 satellites GPS constellation.

A 5 degree mask angle has been used for GPS satellites and a 10 degree mask angle has been used for the Galileo satellites.

These assumptions lead to an average of 17 visible satellites on Earth (see figure 3).

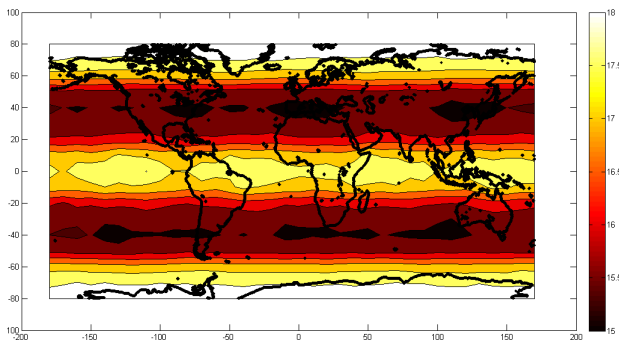


Figure 3-Average number of visible satellites

Only 4 unknowns have been taken for the position solution computation, that is to say that the GPS/Galileo time difference is not considered as an unknown.

I-3-2- Pseudo range measurement error

The pseudo range measurement error variances from different sources are gathered in the User Equivalent Range Error UERE. The contributions that have to be considered are: orbit determination and synchronisation error, troposphere residual error, ionosphere residual error, multipath residual error and receiver noise residual error.

- Receiver noise residual error

Computation of error variance of a code-tracking loop

The error variance of the code-tracking loop will depend on the choice of the discriminator. Assuming that

interference can be assimilated to white noise and for Early Minus Late Power discriminator (for example) [4]:

$$\sigma_{EMLP}^2 = \frac{B_L(1-0.5B_L T) \int_{-B/2}^{B/2} G(f) \sin^2(\pi f C_S) df}{\frac{C}{N_0} \left(2\pi \int_{-B/2}^{B/2} f G(f) \sin(\pi f C_S) df \right)^2} \times \left(1 + \frac{\int_{-B/2}^{B/2} G(f) \cos^2(\pi f C_S) df}{\frac{C}{N_0} T \left(\int_{-B/2}^{B/2} G(f) \cos(\pi f C_S) df \right)} \right), \text{ where}$$

$B_L(H_z)$ the one sided bandwidth of the equivalent loop filter

T the data period

G the power spectrum density of the signal

C/N_0 the signal to noise ratio

C_S the chip spacing

B the two sided bandwidth of the front end filter

Without considering the temporal repetition period of the PN sequence, the power spectrum density expression of the BPSK signal is:

$$G(f) = T_c \left(\frac{\sin \pi f T_c}{\pi f T_c} \right)^2$$

with T_c the code period.

This expression is used for GPS L1, GPS L5 and GALILEO E5b code tracking loop error variance. For Galileo E1, the normalized power spectrum density of the BOC(1,1) is equal to:

$$G(f) = T_c \left(\frac{1 - \cos \pi f T_c}{\pi f T_c} \right)^2$$

The error variance of the code tracking loop, error due to noise, can be thus computed for different kind of signals.

For those simulations, the following values have been used:

	GPS L1	GPS L5	GalileoE1	GalileoE5b
C_S	0.25	0.25	0.25	0.25
B_L	1	1	1	1
B	16	20	20	14
	$\times 10^6 \text{Hz}$	$\times 10^6 \text{Hz}$	$\times 10^6 \text{Hz}$	$\times 10^6 \text{Hz}$
C/N_0	35 dBHz	29 dBHz	36.5 dBHz	29.7 dBHz
T	0.02 s	0.02 s	0.1 s	0.1 s

Note that worst case C/N_0 are considered and not typical values.

Iono free measurements

In nominal mode, the pseudorange measurements that are available to the aircraft receiver are the GPS L1, GPS L5, GALILEO E1, GALILEO E5a, GALILEO E5b code and

phase measurements. But for future civil aviation GNSS receivers complying with EUROCAE requirements, dual frequency measurements will be combined into a single composite measurement called the iono-free measurement, corrected for ionospheric error.

Therefore, from GPS L1 – L5, and from GALILEO E1 – E5b, two distinct iono-free measurements are built.

Denoting $m(k)$ the measurement at the instant k (representing $P(k)$ the code measurement or $\varphi(k)$ the phase measurement):

$$m_{1-5}(k) = \frac{f_1^2}{f_1^2 - f_5^2} m_1(k) + \frac{f_5^2}{f_5^2 - f_1^2} m_5(k)$$

and

$$\begin{aligned} \frac{f_{L1}^2}{f_{L1}^2 - f_{L5}^2} &\approx 2.261, & \frac{f_{L5}^2}{f_{L5}^2 - f_{L1}^2} &\approx -1.261, \\ \frac{f_{E1}^2}{f_{E1}^2 - f_{E5b}^2} &\approx 2.422, & \frac{f_{E5b}^2}{f_{E5b}^2 - f_{E1}^2} &\approx -1.422 \end{aligned}$$

No significant correlation factor can be expected for the noise and multipath error affecting the different measurements made on the four carrier frequencies. This is why the standard deviation of the error affecting the iono-free measurement is modelled as:

$$\begin{aligned} \sigma_{L1-L5} &= \sqrt{2.261^2 \sigma_{L1}^2 + 1.261^2 \sigma_{L5}^2} \\ \sigma_{E1-E5b} &= \sqrt{2.422^2 \sigma_{E1}^2 + 1.422^2 \sigma_{E5}^2} \end{aligned}$$

Smoothing

Once elaborated, these two GPS and GALILEO iono-free measurements are then smoothed to reduce the influence of noise and multipath [6]:

$$\sigma_{\bar{p}}^2 \approx \frac{\sigma_p^2}{2T_{smooth}}$$

where T_{smooth} is the time smoothing constant in seconds

σ_p^2 is the raw code pseudorange measurement error variance

$\sigma_{\bar{p}}^2$ is the smoothed code pseudorange measurement error variance

Finally, the receiver noise residual error variance σ_{noise}^2 is obtained. It corresponds to the receiver noise, thermal noise, inter channel bias and processing error.

- Multipath error

The smoothed multipath error for the airborne equipment is described by:

$$\sigma_{multipath} = 0.3 + 0.53 \exp\left(-\theta/10deg\right)$$

where θ is the elevation angle in degree of the considered satellite. This was validated and adopted for GPS L1 C/A. It is also assumed here for GPS L5, Galileo E1 and E5b although smaller error can be anticipated [7].

- Ionospheric residual error

In the case of a dual frequency receiver with ionospheric correction the ionospheric residual error is not considered as significant:

$$\sigma_{iono} = 0$$

- Tropospheric residual error

The model for the residual error for the tropospheric delay estimate is:

$$\sigma_{tropo} = \frac{1.001}{\sqrt{0.002001 + \sin El}} \times 0.12 m$$

where El is the elevation angle

This model was adopted for GPS L1 C/A and is assumed for GPS L5 and Galileo E1 and E5b.

- User equivalent range error

The User Equivalent Range Error is the value reflecting the error budget and it is based on the computation of the following contributions: orbit determination and synchronisation error, troposphere residual error, ionosphere residual error, multipath residual error and receiver noise residual error.

$$\sigma_{URE}^2 = \sigma_{URA}^2 + \sigma_{air}^2 + \sigma_{multipath}^2 + \sigma_{tropo}^2 + \sigma_{L1/E5bias}^2$$

$$\sigma_{air}^2 = \sigma_{iono}^2 + \sigma_{noise}^2$$

It is supposed that $\sigma_{URA} = 0.75m$ and $\sigma_{L1E5bias} = 0$.

The figure 1 represents the obtained Galileo smoothed iono free UERE for different elevation angles

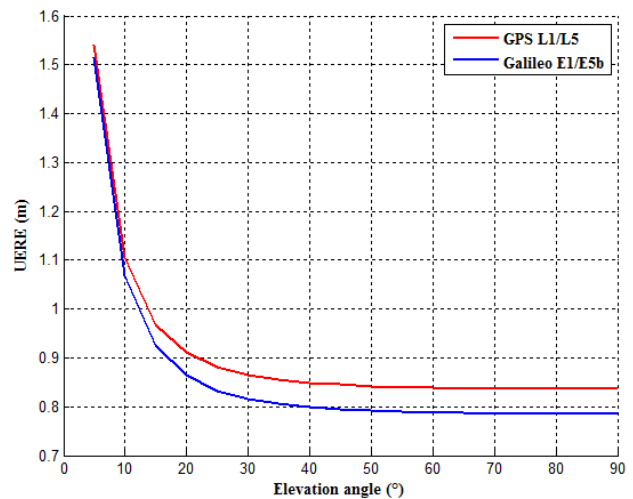


Fig 4– GPS L1/L5 and Galileo E1/E5b smoothed iono-free UERE

Those values are gathered in the following table:

UERE (m)	Elevation angle (°)								
	5	10	15	20	30	40	50	60	90
GPS III L1/L5	1.541	1.105	0.968	0.910	0.865	0.849	0.842	0.839	0.836
Galileo E1/E5b	1.514	1.067	0.925	0.864	0.816	0.799	0.792	0.788	0.785

II- RAIM TECHNIQUES

Two types of RAIM algorithm have been tested in this study: the classical LSR RAIM and the Solution Separation RAIM. The aim of this part is to briefly recall the way they have been implemented for this study.

II-1 LSR RAIM

The classical LSR RAIM method is based on the comparison between a test statistic depending on the prediction error vector and a given threshold.

II-1-1 Implemented Detection function

Let's consider the measurement residual ΔY (also called the prediction error vector) which can be expressed thanks to a linear relationship the measurement error vector E , its covariance matrix Σ and the observation matrix H :

$$\Delta Y = (I - H[H^t \Sigma^{-1} H]^{-1} H^t \Sigma^{-1}) E$$

The LSR RAIM test is then defined by:

$$T = \sqrt{\frac{SSE}{N-4}}$$

where $SSE = \Delta Y^t \cdot \Delta Y = \|\Delta Y\|^2$

The detection threshold is obtained by considering the test statistic in the fault free case

If the measurement error E is noise only such as:

$$E(k) = \begin{bmatrix} n^1(k) \\ \vdots \\ n^j(k) \\ \vdots \\ n^N(k) \end{bmatrix} \text{ with } n^i \sim N(0, \sigma_i^2)$$

Therefore, SSE is chi-squared distributed with $N-4$ degrees of freedom, $SSE \sim \chi_{N-4}^2$, that is to say:

$$\exists X_i, SSE = X_1^2 + \dots + X_{N-4}^2 \text{ iid, } X_i \sim N(0,1)$$

The probability of false alarm is used to determine the normalised detection threshold a such as:

$$P\left(\frac{SSE}{\sigma^2} > a\right) = P_{fa}$$

$$P_{fa} = \int_a^\infty f_{\chi_{N-4}^2(x)} dx$$

where $\sigma = \max_{i \in [1, N]} \sigma_i$

Thus, a fault is detected if the chi-squared variable is abnormally large above the assumed noise level.

Finally, the threshold that it is compared to our criteria is:

$$Th = \sqrt{\frac{a\sigma^2}{N-4}}$$

II-1-1- Protection levels computation

The protection levels derive from the smallest bias the algorithm is able to detect satisfying the false alarm and the missed detection requirement.

Let 's consider that the measurement error E is noise and a bias b on one satellite j such as:

$$E(k) = \begin{bmatrix} n^1(k) \\ \vdots \\ n^j(k) \\ \vdots \\ n^N(k) \end{bmatrix} + \begin{bmatrix} 0 \\ \vdots \\ b \\ \vdots \\ 0 \end{bmatrix}$$

In this case, SSE is chi-squared distributed with $N-4$ degrees of freedom and non-centrality parameter λ such as $SSE \sim \chi_{\lambda, N-4}^2$

$$\exists X_i, SSE = X_1^2 + \dots + X_{N-4}^2 \text{ iid, } X_i \sim N(\mu_i, 1)$$

$$\lambda = \sum_{i=1}^{N-4} \mu_i^2$$

The non centrality parameter λ is computed in order to satisfy the Pmd requirement such as:

$$P_{md} = \int_0^{Th} f_{\chi_{\lambda, N-4}^2(x)} dx$$

The obtained non centrality parameter λ is the smallest that can be detected by the test. It does not depend of any pseudorange.

As $SSE = E^t (I - H[H^t \Sigma^{-1} H]^{-1} H^t \Sigma^{-1}) E = \|\Delta Y\|^2$, the relation between the smallest detectable bias on the pseudorange j and the test statistic is simplified as:

$$\sigma^2 \lambda = b(1 - B_{jj})b = (1 - B_{jj})b^2$$

where $B = H[H^t \Sigma^{-1} H]^{-1} H^t \Sigma^{-1}$

λ is the smallest detectable non-centrality parameter previously obtained

The smallest detectable measurement bias b on satellite j can be then expressed as:

$$b_j = \sigma \sqrt{\frac{\lambda}{1 - B_{jj}}}$$

The relationship between the position error and the measurement error is:

$$X(k) - \hat{X}(k) = -A \times E(k)$$

with $A = [H^t \Sigma^{-1} H]^{-1} H^t \Sigma^{-1}$

Therefore the impact of the bias b_j in position domain is obtained by:

$$\Delta X = X(k) - \hat{X}(k) = \begin{bmatrix} \dots & A_{N,jj} & \dots \\ \dots & A_{E,jj} & \dots \\ \dots & A_{D,jj} & \dots \\ \dots & A_{T,jj} & \dots \end{bmatrix} \times \begin{bmatrix} 0 \\ b_j \\ \vdots \\ 0 \end{bmatrix}$$

Then,

$$\Delta X_H = \sqrt{\Delta X_H^2 + \Delta X_E^2} = \sqrt{A_{N,jj}^2 + A_{E,jj}^2} \times b_j$$

$$\Delta X_V = A_{V,jj} \times b_j$$

Denoting $p_{bias} = \sigma \times \sqrt{\lambda}$, we obtain

$$\Delta X_H = \frac{\sqrt{A_{N,jj}^2 + A_{E,jj}^2}}{\sqrt{1 - B_{jj}}} \times p_{bias}$$

$$\Delta X_V = \frac{|A_{V,jj}|}{\sqrt{1 - B_{jj}}} \times p_{bias}$$

Denoting,

$$VSLOPE_j = \frac{A_{V,jj}}{\sqrt{1 - B_{jj}}}, HSLOPE_j = \frac{\sqrt{A_{N,jj}^2 + A_{E,jj}^2}}{\sqrt{1 - B_{jj}}}$$

The protection levels are computed referring to the worst satellite:

$$HSLOPE_{max} = \max_j (HSLOPE_j)$$

$$VSLOPE_{max} = \max_j (VSLOPE_j)$$

And

$$HPL = HSLOPE_{max} \times p_{bias}$$

$$VPL = VSLOPE_{max} \times p_{bias}$$

II-2 Solution Separation RAIM

The solution separation method is based on the observed separation between the position estimate generated by the full-set filter (using all the satellite measurements) and that generated by each one of the subset filters (each using all but one of the satellite measurements).

The separation d_i between each pair of the estimates (the full filter estimate and each sub-filter estimate) forms a test statistic and each test statistic is compared to its

respective detection threshold D_i which is determined to meet the maximum allowable rate requirement

II-2-1 Implemented detection function

Let $X(k)$ be the true user position at the instant k and $\hat{X}(k)$ the LSR user position estimation at the instant k

Then the relationship between the position error and the measurement error is:

$$X(k) - \hat{X}(k) = -A \times E(k)$$

with $A = [H^t \Sigma^{-1} H]^{-1} H^t \Sigma^{-1}$

For $i \in [1, N]$, let $\hat{X}_i(k)$ be the LSR user position estimation at the instant k do not considering the pseudo range obtained from the satellite i .

The solution separation discriminators are 4×1 vectors linearly depending on the error measurement such as:

$$d_i(k) = \hat{X}(k) - \hat{X}_i(k) = (A_i - A) \times E(k)$$

Their covariance matrix is given by:

$$dP_i(k) = (A_i - A) \Sigma (A_i - A)^t$$

For the horizontal part, computations that are not described here show that for the criteria $d_{i,H}$ where $i \in [1, N]$ a threshold D_i satisfying the probability of false alarm can be defined such as:

$$D_i = \sqrt{\lambda_i} Q^{-1} \left(\frac{P_{fa}}{2N} \right)$$

where $Q(x) = \frac{1}{\sqrt{2\pi}} \int_x^\infty e^{-\frac{t^2}{2}} dt$

λ_i is the largest eigenvalue of the covariance matrix $dP_{i,H} = dP_i(1:2, 1:2)$

For the vertical part of the detection, we obtain for $i \in [1, N]$ the threshold V_i such as:

$$1 - \frac{P_{fa}}{2N} = \frac{1}{\sqrt{2\pi}\sigma_v} \int_{-\infty}^{V_i} e^{-\frac{t^2}{2\sigma_v^2}} dt$$

Or such as

$$\frac{P_{fa}}{2N} = \frac{1}{\sqrt{2\pi}\sigma_v} \int_{V_i}^\infty e^{-\frac{t^2}{2\sigma_v^2}} dt$$

where $\sigma_v^2 = dP_i(3,3)$

II-2-2 Protection level computation

For $i \in [1, N]$, let's assume that there is a bias b_i on the pseudorange i and that it is not detected by the corresponding criteria.

For the horizontal aspect that means that:

$$\|\hat{X}_{H,i} - \hat{X}_{H,0}\| \leq D_i$$

Since $X - \hat{X}_0 = X - \hat{X}_i + \hat{X}_i - \hat{X}_0$:

$$\|X - \hat{X}_0\| \leq \|X - \hat{X}_i\| + \|\hat{X}_i - \hat{X}_0\|$$

Therefore, $\|X - \hat{X}_0\| \leq \|X - \hat{X}_i\| + D_i$

Since the faulty measurement has been removed from \hat{X}_i computation, the vector $X - \hat{X}_i$ corresponds to a fault free case situation.

So let's consider the distribution of this vector $\Delta\hat{X}_i = X - \hat{X}_i$ which is the position error resulting from the sub solution that doesn't take into account the i^{th} pseudorange

Computations that are not described here show that in this case $\|\Delta\hat{X}_i\|$ is bounded by $\delta_i = \sqrt{-2\ln(p)} \times \sqrt{\mu_i}$ with the probability $1 - p$

Therefore,

$$p \left(\begin{array}{l} \|X - \hat{X}_0\| \leq \delta_i + D_i / \exists \text{ non detected} \\ \text{bias on the } i^{th} \text{ pseudorange} \end{array} \right) \leq 1 - p$$

And a class of horizontal protection levels can be defined as:

$$HPL = \max_{i \in [1, N]} (\delta_i + D_i)$$

For the vertical aspect, $|\hat{X}_{V,i} - \hat{X}_{V,0}| \leq V_i$ and $|X_V - \hat{X}_{V,i}|$ can be easily bounded with the probability $1 - p$.

A bound γ_i is obtained such as

$$p = \frac{1}{\sqrt{2\pi}\sigma_v} \int_{-\gamma_i}^{\gamma_i} e^{\frac{-t}{2\sigma_v^2}} dt$$

A class of vertical protection levels can be defined as:

$$VPL = \max_{i \in [1, N]} (\gamma_i + V_i)$$

III- SIMULATIONS RESULTS

III-1 LSR RAIM

1- Protection level

Vertical and horizontal protection levels have been computed for each point of our user grid.

As it can be seen on the following figures the protection are much lower than the corresponding alert limit. It results that the LSR RAIM is 100% of the time available for APVI operation for each point of our user grid.

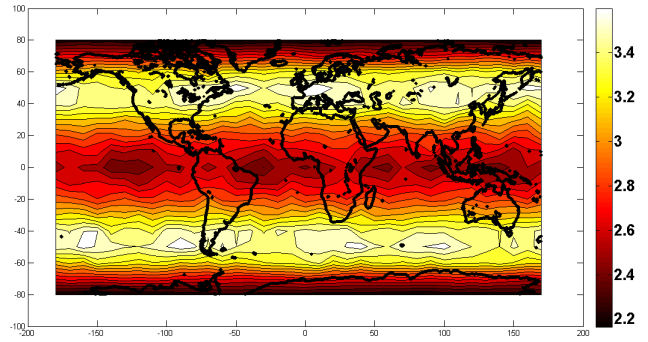


Figure 5- Horizontal Protection Level

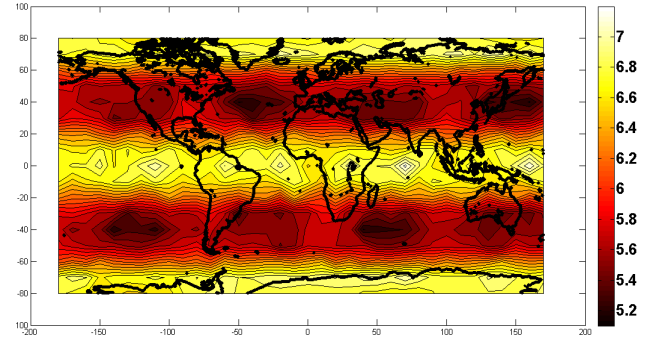


Figure 6- Vertical Protection Level

2- Monte-Carlo simulations

Monte Carlo simulations have been performed by adding on each available pseudorange the smallest bias that will lead to a positioning failure. The algorithm ability to detect it has been measured.

For every user position at every epoch of 3-days simulation period, biases have been successively added on each available smoothed GPS L1/L5 or Galileo E1/E5b.pseudorange measurement. Only one critical bias was added at the same time on the measurements. For each pseudorange, the number of simulation iteration has been designed to be significant with respect to required probability of missed detection such as: $n_{iter} \approx 10^{P_{md}^{-1}}$

The way this critical bias is computed for every pseudorange is detailed in appendix. The average value of this critical bias is represented on the following figure:

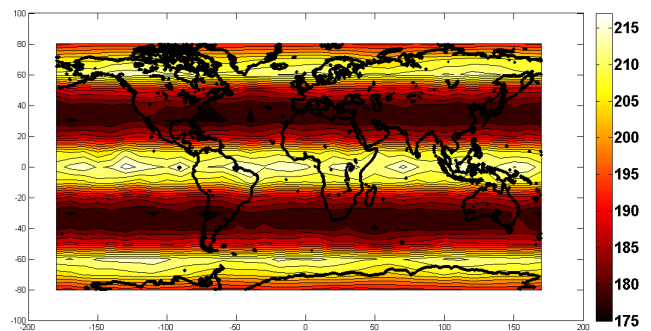


Figure 7- Average critical bias

These simulations have demonstrated that the implemented classical LSR RAIM was always able to detect the smallest dangerous biases showing an availability of 100% for APVI operation for each point of our user grid.

III-2 Solution Separation RAIM

Vertical and horizontal protection levels have been computed for each point of our user grid.

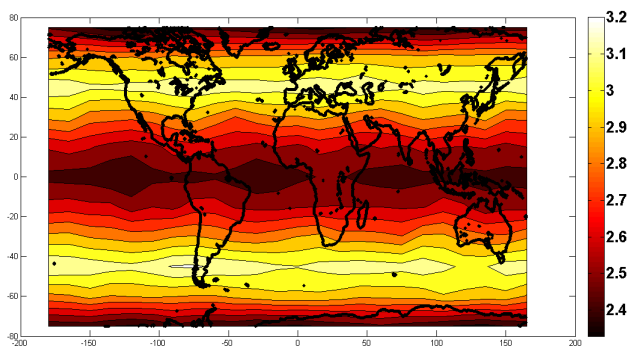


Figure 8- Horizontal Protection Level

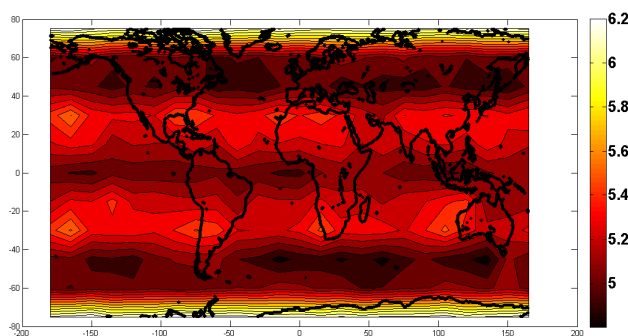


Figure 9- Vertical Protection Level

As it can be seen the protection levels are much lower than the corresponding alert limit. It results that the Solution Separation RAIM is 100% of the time available for APVI operation for each point of our user grid.

CONCLUSION

A complete review of the assumptions that are made in RAIM simulations has been first proposed in this paper.

It has been demonstrated, for the single failure case using GPS + Galileo constellations, that the amplitude of pseudo range additional biases that lead to a positioning failure are systematically larger than 30 meters for APV I operations. Therefore even if the targeted phases of flight are characterized by smaller horizontal and vertical tolerable position errors compared to NPA, this effect is mitigated by the great number of available measurements that reduce the impact of a single satellite bias on the global positioning error. Thus only Major Service Failures are taken into account for the single failure case in this study.

It also has been seen that the improvement in the quality of measurements (dual frequency measurements, better clock and ephemeris information, better ranging signals) has significantly decreased the user equivalent range error variance. Considering that UERE is the major parameter of position estimation and autonomous integrity monitoring performance, great RAIM availability could be expected from an UERE standard deviation of approximately one meter.

Then classical LSR and Solution Separation RAIM availabilities have been computed for APVI approaches using both GPS L1/L5 and Galileo E1/E5b pseudorange measurements. An availability of 100% has been obtained for the both algorithms. For the LSR RAIM and the Solution Separation RAIM, all computed xPL were below the corresponding xAL for every point of the user grid and for each epoch. Moreover, the LSR RAIM has been able to detect every single critical bias that has been added on each available pseudorange.

Nevertheless the threat model that has been used in this study still needs to be consolidated since it does not consider the multiple failure case. Even for the single failure case, the threat model should be completed in order to take into account potential nominal biases due to signal deformation and antenna bias. These nominal biases are not correctly bounded with zero-mean Gaussian distributions which are currently used for modeling the error measurement in the fault free case. This parameter should be included in future protection level calculation.

Concerning the detection of multiple failures, Solution Separation RAIM algorithm seems to be a promising method but complete studies need to be conducted using a consolidated threat model.

It is also important to keep in mind that only integrity aspects have been addressed through this paper. Continuity issue also needs to be studied before considering RAIM as a future mean for performing integrity monitoring in APV operations.

Thus, further studies are needed to definitively conclude on the potential use of RAIM for approaches with vertical guidance even if these results seem promising.

APPENDIX: CRITICAL BIAS

This part is dedicated to the computation for each pseudo range i of the bias b_i that will lead to a positioning failure with a probability corresponding to the integrity risk.

Let us consider the case where there is a bias on the pseudo range i ,

The error in the position domain is:

$$\epsilon_{pos,WGS84} = (H' \Sigma^{-1} H)^{-1} H' \Sigma^{-1} (\xi + B)$$

where $\xi \sim N(0_{4 \times 1}, \Sigma)$ and $B = \begin{bmatrix} 0 \\ \vdots \\ b_i \\ \vdots \\ 0 \end{bmatrix}$

If the matrix H is expressed in the local geographic frame such as:

$$H = \begin{bmatrix} \cos E_i \cos A_i & \cos E_i \sin A_i & \sin E_i & 1 \\ \vdots & \vdots & \vdots & \vdots \\ \vdots & \vdots & \vdots & \vdots \\ \cos E_n \cos A_n & \cos E_n \sin A_n & \sin E_n & 1 \end{bmatrix}$$

Then the positioning error is directly expressed in the local geographic frame

$$\mathcal{E}_{pos,local} = (H^T \Sigma^{-1} H)^{-1} H^T \Sigma^{-1} (\xi + B)$$

The covariance matrix C of the error is such as:

$$\begin{aligned} C &= E[\mathcal{E}_{pos,local} \mathcal{E}_{pos,local}^T] \\ &= \left((H^T \Sigma^{-1} H)^{-1} H^T \Sigma^{-1} \right) \Sigma \left((H^T \Sigma^{-1} H)^{-1} H^T \Sigma^{-1} \right)^T \\ &= (H^T \Sigma^{-1} H)^{-1} \end{aligned}$$

The horizontal positioning error is a two dimensions vector which follows a Gaussian bi-dimensional law of mean $b_{i,local,H}$ the projection of b_i in the horizontal plane and of covariance matrix C_H , such as $C_H = C(1:2,1:2)$, $b_{i,local} = (H^T \Sigma^{-1} H)^{-1} H^T \Sigma^{-1}$ and $b_{i,local,H} = b_{i,local}(1:2)$

Its density function is:

$$f_{\mathcal{E}_{pos,local}}(X) = \frac{1}{2\pi\sqrt{\det C_H}} \exp\left(-\frac{1}{2}(X - b_{i,local,H})^T C_H^{-1} (X - b_{i,local,H})\right)$$

where X is expressed in the Nord East local frame such as

$$X = \begin{bmatrix} x_N \\ x_E \end{bmatrix}$$

Since C_H is a covariance matrix, C_H is a positive definite matrix, it is diagonalizable and its eigenvalues are all positive. In particular we can find an orthonormal basis $B = (\vec{e}_1, \vec{e}_2)$ that is composed of eigenvectors $\vec{e}_{1,i}, \vec{e}_{2,i}$ corresponding to the eigenvalues λ_1 and λ_2 and such as:

$$C_H = P_{\perp} \cdot \Delta \cdot P_{\perp}^T$$

where,

- $\Delta = \text{diag}(\lambda_1, \lambda_2)$ is the diagonal matrix whose elements are the eigenvalues of C_H
- P_{\perp} is the projection matrix whose columns are the eigenvectors \vec{e}_1, \vec{e}_2 . In particular P_{\perp} is orthogonal: $P_{\perp}^{-1} = P_{\perp}^T$.

Then we have $\det(C_H) = \lambda_1 \lambda_2$,

$$C_H^{-1} = P_{\perp} \cdot \Delta^{-1} \cdot P_{\perp}^T$$

$$\begin{aligned} & (X - b_{i,local,H})^T C_H^{-1} (X - b_{i,local,H}) \\ &= (X - b_{i,local,H})^T P_{\perp} \cdot \Delta^{-1} \cdot P_{\perp}^T (X - b_{i,local,H}) \\ &= [P_{\perp}^T (X - b_{i,local,H})]^T \cdot \Delta^{-1} \cdot [P_{\perp}^T (X - b_{i,local,H})] \end{aligned}$$

And we have $X_{\perp} = P_{\perp}^T X$ and $\Omega = P_{\perp}^T b_{i,local,H}$ X_{\perp} where is the vector X expressed in the new local frame and Ω is the vector $b_{i,local,H}$ in the new local frame.

$$f_0(X) = \frac{1}{2\pi\sqrt{\lambda_1\lambda_2}} \exp\left(-\frac{1}{2}\left(\frac{(x_{\perp} - \Omega_1)^2}{\lambda_1} + \frac{(y_{\perp} - \Omega_2)^2}{\lambda_2}\right)\right)$$

The probability that a couple (x, y) be such that $x^2 + y^2 \leq HAL^2$ is the probability that $x_{\perp}^2 + y_{\perp}^2 \leq HAL^2$ and considering the distribution of the horizontal positioning error, this probability is:

$$P(X \in D) = \iint_D \frac{1}{2\pi\sqrt{\lambda_1\lambda_2}} \exp\left(-\frac{1}{2}\left(\frac{(x_{\perp} - \Omega_1)^2}{\lambda_1} + \frac{(y_{\perp} - \Omega_2)^2}{\lambda_2}\right)\right) dx dy$$

denoting D the domain such as $x_{\perp}^2 + y_{\perp}^2 \leq HAL^2$.

Let's make a change of coordinates such as we could

have $\frac{(x_{\perp} - \Omega_1)^2}{\lambda_1} + \frac{(y_{\perp} - \Omega_2)^2}{\lambda_2} = r^2$. We re-write

(x_{\perp}, y_{\perp}) this way:

$$\begin{cases} x_{\perp} = \Omega_1 + r\sqrt{\lambda_1} \cos \theta \\ y_{\perp} = \Omega_2 + r\sqrt{\lambda_2} \sin \theta \end{cases}$$

The equation $x_{\perp}^2 + y_{\perp}^2 = HAL^2$ that defines the boundaries of the integration domain becomes:

$$x_{\perp}^2 + y_{\perp}^2 = (\Omega_1 + r\sqrt{\lambda_1} \cos \theta)^2 + (\Omega_2 + r\sqrt{\lambda_2} \sin \theta)^2$$

$$= \Omega_1^2 + r^2 \lambda_1 \cos^2 \theta + 2\Omega_1 r \sqrt{\lambda_1} \cos \theta + \Omega_2^2 + r^2 \lambda_2 \sin^2 \theta + 2\Omega_2 r \sqrt{\lambda_2} \sin \theta = HAL^2$$

$$r^2 (\lambda_1 \cos^2 \theta + \lambda_2 \sin^2 \theta) + r (2\Omega_1 \sqrt{\lambda_1} \cos \theta + 2\Omega_2 \sqrt{\lambda_2} \sin \theta) + (\Omega_1^2 + \Omega_2^2 - HAL^2) = 0$$

Solving this equation, two roots $r_1(\theta)$ and $r_2(\theta)$ for $\theta \in [0, \pi]$ are obtained such as:

$$\begin{cases} x_{\perp} = \Omega_1 + r_1(\theta) \sqrt{\lambda_1} \cos \theta \\ y_{\perp} = \Omega_2 + r_1(\theta) \sqrt{\lambda_2} \sin \theta \end{cases} \quad \text{and} \quad \begin{cases} x_{\perp} = \Omega_1 + r_2(\theta) \sqrt{\lambda_1} \cos \theta \\ y_{\perp} = \Omega_2 + r_2(\theta) \sqrt{\lambda_2} \sin \theta \end{cases} \quad \text{define the}$$

boundaries of the integration domain.

The jacobian of this transformation is computed to make our change of coordinates $J = |r| \sqrt{\lambda_1 \lambda_2}$, and:

$$P(X_H \in D) = \iint_{D'} \frac{|r|}{2\pi} \exp\left(-\frac{r^2}{2}\right) dr d\theta$$

where the new domain D' is defined by

$$\begin{cases} (r - r_1(\theta))(r - r_2(\theta)) \leq 0 \\ \theta \in [0, \pi] \end{cases}$$

Considering properties of second order polynomials:

$$P(X_H \in D) = \frac{1}{2\pi} \int_{\theta=0}^{\theta=\pi} \int_{r=r_1(\theta)}^{r=r_2(\theta)} |r| \exp\left(-\frac{r^2}{2}\right) dr d\theta$$

Assuming for example that $r_1 \leq 0 \leq r_2$,

$$P(X_H \in D) = \frac{1}{2\pi} \times \int_{\theta=0}^{\theta=\pi} \left[- \int_{r=r_2}^{r=0} r \exp\left(-\frac{r^2}{2}\right) dz + \int_{r=0}^{r=r_1} r \exp\left(-\frac{r^2}{2}\right) dr \right] d\theta$$

$$P(X_H \in D) = 1 - \frac{1}{2\pi} \int_{\theta=0}^{\theta=\pi} \left[\exp\left(-\frac{r_2^2}{2}\right) + \exp\left(-\frac{r_1^2}{2}\right) \right] d\theta$$

and this last integral is computed numerically.

Thus the probability that the point (x, y) is out of the circle of radius HAL is:

$$P(X_H \notin D) = \frac{1}{2\pi} \int_{\theta=0}^{\theta=\pi} \left[\exp\left(-\frac{r_2^2}{2}\right) + \exp\left(-\frac{r_1^2}{2}\right) \right] d\theta$$

In order to pass from a bias b on a given pseudo range to an error vector in the local horizontal plane, projections are made using linear relations. Denoting

$$A = (H^T H)^{-1} H^T \quad \text{we define for } i \in [1, N]:$$

$$H_{pseudo_pos_North}(i) = |A_{1,i}|$$

$$\text{and} \quad H_{pseudo_pos_East}(i) = |A_{2,i}|$$

An equivalent analysis of the vertical risk (which is easier in one dimension) must also be done. Then by comparing successively the obtained probabilities with the integrity risk for different bias amplitudes, the minimum bias which leads to a positioning failure with a probability equal to the integrity risk is finally obtained.

REFERENCES

- [1] Global Positioning System Standard Positioning Service Signal Specification (1995), Second Edition, June 1995
- [2] RTCA/ DO 245A (2004), "Minimum Aviation System Performance Standards for Local Area Augmentation System (LAAS)", RTCA, Inc., Washington D.C., USA.
- [3] RTCA/ DO 229D (2006), "Minimum Operational Performance Standards for Global Positioning Systems / Wide Area Augmentation System Airborne Equipment", RTCA, Inc., Washington D.C., USA.
- [4] Hegarty C. (1996), "Analytical Derivation of Maximum Tolerable In-Band Interference Level for Aviation Applications of GNSS"
- [5] Julien O. (2005), "Design of Galileo L1F tracking loops", Ph.D. thesis, University of Calgary, Department of Geomatics Engineering
- [6] Martineau, A., C. Macabiau, (2008), "Computation of the smallest bias that lead to a positioning failure", ENAC internal report
- [7] Macabiau, C. (2007), "GNSS Integrity Course", GNSS Solutions Tutorials ION GNSS 2007
- [8] Macabiau C., L. Moriella, M. Raimondi, C. Dupouy, A. Steingass, A. Lehner (2006), "GNSS Airborne Multipath Errors Distribution Using the High Resolution Aeronautical Channel Model and Comparison to SARPs Error Curve", ION NTM 2006, January.
- [9] Brown R. G., G. Y. Chin (1997), "GPS RAIM: calculation of threshold and protection radius using chi-square methods – a geometric approach", Global Positioning System: Institute of Navigation, vol. V, pp. 155–179, 1998
- [10] Brenner M. (1990), "Implementation of a RAIM Monitor in a GPS Receiver and an Integrated GPS/IRS", ION 1990
- [11] Brenner M. (1996), "Integrated GPS/inertial detection availability", Journal of The Institute of Navigation, Vol. 43, No. 2, Summer 1996